

# Beyond 2-to-2: Geometrization of Entanglement Wedge Connectivity in Holographic Scattering

---

**Bowen Zhao**

*Beijing Institute of Mathematical Sciences and Applications, Beijing, China*

*E-mail:* [bowenzhao@bimsa.cn](mailto:bowenzhao@bimsa.cn)

**ABSTRACT:** We extend recent discussions on generalization of the Connected Wedge Theorem about 2-to-2 holographic scattering problem to  $n$ -to- $n$  scatterings ( $n > 2$ ). In this broader setting, our theorem provides a weaker necessary condition for the connectedness of boundary entanglement wedges than previously identified. Besides, we prove a novel sufficient condition for this connectedness. We also present an analysis of the criteria ensuring a non-empty entanglement wedge intersection region  $\mathcal{S}_E$ . These results refine the holographic dictionary between geometric connectivity and quantum entanglement for general multi-particle scattering.

**KEYWORDS:** AdS/CFT Correspondence, Holographic Entanglement Entropy, Entanglement Wedge, Scattering Amplitudes, Superadditivity

---

## Contents

<b>1</b>	<b>Introduction</b>	<b>1</b>
1.1	Notations and Assumptions	3
<b>2</b>	<b>Review and Preliminary</b>	<b>4</b>
2.1	Boundary setup of n-to-n scattering	4
2.2	Causal Anchoring Principle	6
2.3	Intersections among wedge horizons	6
2.4	Characterization of connected entanglement wedges	10
<b>3</b>	<b>Generalizing the n-to-n Connected Wedge Theorem</b>	<b>12</b>
3.1	An improvement of the n-to-n Connected Wedge Theorem	12
3.2	Consequences of connected entanglement wedges	16
3.2.1	Consequence from a connected–disconnected area comparison	16
3.2.2	Consequences from pairwise consideration	17
3.2.3	A layered reduction from pairwise data to a top-level entering ridge	21
3.3	Generalized bulk scattering regions	23
<b>4</b>	<b>Conclusion and Discussion</b>	<b>24</b>
4.1	An observation about different generalizations of the 2-to-2 Connected Wedge Theorem	24
4.2	Future Directions	26

---

## 1 Introduction

The AdS/CFT correspondence posits a duality between a quantum gravity theory in an asymptotically Anti-de Sitter (AdS) spacetime  $M$  and a conformal field theory (CFT) on its timelike boundary  $\partial M$  [1, 2]. A foundational requirement of the correspondence is the consistency of causal structure between the bulk and the boundary. Gao and Wald proved that, assuming the null curvature condition and global hyperbolicity, bulk causality cannot violate boundary causality: if two boundary points are connected by a causal curve through the bulk, they are also connectable by a causal curve restricted to the boundary [3].

A more subtle consistency requirement emerges for asymptotic quantum tasks involving multiple boundary regions. Consider an asymptotic  $n$ -to- $n$  scattering configuration on the boundary  $\partial M$ , specified by  $n$  disjoint input regions  $V_1, \dots, V_n$  and  $n$  disjoint output regions  $W_1, \dots, W_n$ . Local scattering processes can occur in the bulk that have no direct boundary counterpart, referred to as *bulk-only scattering* [4–7].

For the 2-to-2 case ( $n = 2$ ), the Connected Wedge Theorem (CWT) [8] establishes that for such a bulk-only process, the associated boundary input regions  $V_1$  and  $V_2$  must

share  $O(1/G_N)$  mutual information,  $I(V_1 : V_2) \sim O(1/G_N)$ . This implies that a local bulk scattering process necessitates nonlocal boundary protocols.

Via the Hubeny–Rangamani–Ryu–Takayanagi (HRRT) prescription [9, 10], this large mutual information admits a geometric interpretation: the entanglement wedge of  $V_1 \cup V_2$  becomes connected. Under standard assumptions (AdS hyperbolicity, the null curvature condition, and the maximin construction for HRRT surfaces), the CWT may be stated geometrically [8]:

**Theorem 1.1.** *Under standard assumptions, for a 2-to-2 bulk-only scattering configuration, the entanglement wedge of  $V_1 \cup V_2$  is connected.*

Recent works have elevated the Connected Wedge Theorem to a precise equivalence [11, 12]. They show that the existence of  $O(1/G_N)$  mutual information between the two input regions  $V_1$  and  $V_2$  is equivalent to the non-emptiness of a generalized bulk scattering region, denoted  $\tilde{S}_E$ . This region is defined as the intersection of the entanglement wedge of the union of input regions (with the wedges of individual input regions removed) and the entanglement wedge of the union of output regions (with the wedges of individual output regions removed). This provides a complete geometric characterization of quantum nonlocal scattering in the 2-to-2 case. We refer the reader to [11] for a comprehensive review.

In this paper, we extend these analyses to general asymptotic  $n$ -to- $n$  scattering processes with  $n > 2$ . A necessary condition for the connectedness of the input entanglement wedge  $\mathcal{E}(V_1 \cup \dots \cup V_n) := \mathcal{E}(V_1 \cup \dots \cup V_n)$  was previously derived in Ref. [13]:

**Theorem 1.2.** *Under standard assumptions, if the 2-to-all graph  $\Gamma_{2 \rightarrow \text{all}}$  is connected, then the entanglement wedge  $\mathcal{E}(V_1 \cup \dots \cup V_n)$  is connected.*

The 2-to-all graph  $\Gamma_{2 \rightarrow \text{all}}$  has vertices  $\{1, \dots, n\}$  corresponding to the input regions  $V_1, \dots, V_n$ . An edge between vertices  $i$  and  $j$  is inserted if

$$J^+[\mathcal{E}(V_i)] \cap J^+[\mathcal{E}(V_j)] \cap \bigcap_{k=1}^n J^-[\mathcal{E}(W_k)] \neq \emptyset. \quad (1.1)$$

Our first contribution is to establish a strictly weaker necessary condition for the connectedness of  $\mathcal{E}(V_1 \cup \dots \cup V_n)$  than Theorem 1.2. Specifically, we show that the existence of a *single* suitable pair of input regions already suffices:

**Theorem 1.3.** *Assume the standard conditions listed in Assumption 1. If there exists a pair  $i \neq j$  such that*

$$J^+[\mathcal{E}(V_i)] \cap J^+[\mathcal{E}(V_j)] \cap \bigcap_{k=1}^n J^-[\mathcal{E}(W_k)] \neq \emptyset, \quad (1.2)$$

*then the entanglement wedge  $\mathcal{E}(V_1 \cup \dots \cup V_n)$  is connected.*

The proof reveals an even weaker condition than (1.2), albeit one with a less transparent physical interpretation.

We then derive new, independent *sufficient* conditions for the connectedness of multipartite entanglement wedges. In particular, we show that when both the input wedge  $\mathcal{E}(V_1 \cup \dots \cup V_n)$  and the output wedge  $\mathcal{E}(W_1 \cup \dots \cup W_n) := \mathcal{E}(W_1 \cup \dots \cup W_n)$  are connected, one necessarily finds a pair of enlarged output regions whose entanglement wedge intersects  $\mathcal{E}(V_1 \cup \dots \cup V_n)$ . A complete statement is given in Theorem 3.2.

Finally, motivated by the central role of the entanglement wedge intersection  $\mathcal{S}_E = \mathcal{E}(V_1 \cup V_2) \cap \mathcal{E}(W_1 \cup W_2)$  in the 2-to-2 case, we analyze its generalization to  $n$ -to- $n$  processes. We provide a necessary condition for  $\mathcal{S}_E = \mathcal{E}(V_1 \cup \dots \cup V_n) \cap \mathcal{E}(W_1 \cup \dots \cup W_n) \neq \emptyset$  (Theorem 3.4). Our results indicate that for  $n > 2$ , the existence of a nontrivial  $\mathcal{S}_E$  is governed by constraints stronger than simple connectedness of the input and output wedges, reflecting the intrinsically multipartite nature of the problem.

The paper is organized as follows. Section 2.1 reviews the geometric setup for asymptotic  $n$ -to- $n$  scattering on the boundary  $\partial M$ . Section 2.2 recalls the causal anchoring principle. Section 2.3 summarizes key geometric results concerning intersections of bulk causal boundaries and introduces the geometric ordering of ridges. Section 2.4 reviews criteria for connectedness and disconnectedness of multipartite entanglement wedges. Our results on necessary and sufficient conditions for the connectedness of  $\mathcal{E}(V_1 \cup \dots \cup V_n)$  are presented in Sections 3.1 and 3.2, respectively. Section 3.3 discusses conditions under which the generalized scattering region  $\mathcal{S}_E$  is nonempty. We conclude with a discussion in Section 4. In particular, Section 4.1 compares different null-sheet constructions used in the literature.

### 1.1 Notations and Assumptions

Here we summarize the notations, conventions, and assumptions used throughout this paper.

We adopt natural units with  $\hbar = c = 1$  and set the AdS length scale  $l_{\text{AdS}} = 1$ , while keeping Newton's constant  $G_N$  explicit. Our notation follows ref. [14], using the mostly-plus metric signature.

- **Spacetime regions:** Bulk regions are denoted by script letters  $(\mathcal{U}, \mathcal{V}, \mathcal{W}, \dots)$ , while boundary regions use straight capitals  $(U, V, W, \dots)$ . The same symbol may denote either a causal diamond or its Cauchy surface, with the meaning clear from context.
- **Cauchy slices:** Bulk Cauchy slices are denoted by  $\Sigma$  with appropriate subscripts, boundary Cauchy slices by  $\hat{\Sigma}$  with subscripts. By abuse of notation,  $\Sigma$  may also refer to Cauchy slices of the conformally compactified spacetime.
- **Causal structure:** The bulk causal future/past of region  $\mathcal{V}$  is  $J^\pm[\mathcal{V}]$ ; for boundary region  $V$ , we write  $J^\pm[V]$  for bulk causal influence and  $\hat{J}^\pm[V]$  for boundary causal influence.
- **Domains of dependence:** The bulk domain of dependence of  $\mathcal{V}$  is  $\mathcal{D}[\mathcal{V}]$ ; the boundary domain of dependence of  $V$  is  $\hat{D}[V]$ . The future and past horizons of a causal domain  $V$  is  $\hat{H}^\pm[V]$ .

- **Entanglement structures:** For boundary region  $V$ , we denote the entanglement wedge by  $\mathcal{E}(V)$ , causal wedge by  $\mathcal{C}(V)$ , and HRRT surface by  $\text{RT}(V)$ .
- **Complements:** The causal complement (bulk or boundary) uses superscript  $c$ , while set-theoretic complement within a Cauchy slice uses superscript prime notation  $(')$ .

**Assumption 1.** *We assume throughout that:*

1. *The bulk spacetime  $M$  satisfies the null curvature condition;*
2. *HRRT surfaces can be found via a maximin procedure;*
3. *The spacetime is AdS-hyperbolic (the conformal compactification  $\overline{M} = M \cup \partial M$  admits a Cauchy slice);*
4. *The spacetime region between some Cauchy slice preceding  $\mathcal{E}(V_1 \cup V_2)$  and some Cauchy slice following  $\mathcal{E}(W_1 \cup W_2)$  is singularity-free.*
5. *The global boundary state is pure, ensuring that a boundary region  $V$  and its causal complement  $V'$  share the same HRRT surface.*

## 2 Review and Preliminary

### 2.1 Boundary setup of n-to-n scattering

The set-up of  $n$ -to- $n$  asymptotic scattering is discussed in detail in ref. [13]. We summarize the setup here with a slightly different formulation.

The boundary configuration for the  $n$ -to- $n$  scattering process consists of input points  $c_1, c_2, \dots, c_n$  and output points  $r_1, r_2, \dots, r_n$ . Let  $\hat{\Sigma}_1$  be a boundary spacelike Cauchy slice containing all  $c_i$ 's and let  $\hat{\Sigma}_2$  be a boundary spacelike Cauchy slice containing all  $r_j$ 's. A case of  $n = 3$  is shown in Figure 1 for illustration.

Recall that the input/decision regions and output regions are defined as

$$\begin{aligned} V_i &= \hat{J}^+[c_i] \cap \hat{J}^-[r_1] \cap \dots \cap \hat{J}^-[r_n], \\ W_i &= \hat{J}^-[r_i] \cap \hat{J}^+[c_1] \cap \dots \cap \hat{J}^+[c_n] \end{aligned}$$

which are all non-empty sets on  $\partial M$  by construction. That is, each input  $c_i$  can causally signal all outputs and each output  $r_i$  can be causally signaled by all inputs  $c_i$ . Meanwhile, we require pairwise intersection among these input and output regions to be empty, i.e.

$$\begin{aligned} V_i \cap V_j &= \emptyset, & W_i \cap W_j &= \emptyset, & \forall i \neq j \\ V_i \cap W_j &= \emptyset, & \forall i, j \end{aligned} \tag{2.1}$$

That is, we require 2-to- $n$  and  $n$ -to-2 scattering regions to be empty on  $\partial M$ .

We will show that these requirements force the null rays from  $c_i$ 's and  $r_j$ 's to form a lattice on  $\partial M$ . To explain this, we label future antipodal points of  $c_i$  by  $\alpha_i$  and past antipodal points of  $r_j$  by  $\beta_j$ . For example,  $\alpha_1$  is the future antipodal point of  $c_1$  on  $\partial M$ .

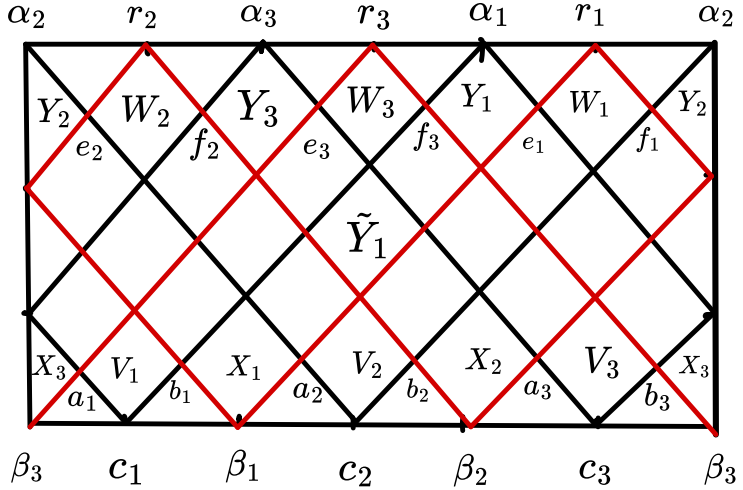


**Figure 1.** Boundary set-up of 3-to-3 scattering process. Points  $c_1, \dots, c_n$  denote inputs while points  $r_1, \dots, r_n$  denote outputs. The point  $\alpha_i$  is the conjugate point of  $c_i$  while the point  $\beta_j$  is the conjugate point of  $r_j$ . Input regions  $V_i$ , with spacelike boundary points  $a_i$  and  $b_i$ , and output regions  $W_j$ , with spacelike boundary points  $e_j$  and  $f_j$ , are also shown. The causal domain  $\tilde{Y}_1$  is marked for later reference.

That is, the two future-directed null geodesics emanating from  $c_1$  converge at  $\alpha_1$ . Similarly, the two past-directed null geodesics from  $r_j$  converge at  $\beta_j$ .

To start with, we label  $c_i$  and  $r_j$  such that the number increases to the right, or  $c_1, \dots, c_n$  and  $r_1, \dots, r_n$  are ordered counterclockwise when viewed from the future. Since the boundary is topologically  $S^1 \times \mathbb{R}^1$ , we always count modulo  $n$ ; that is,  $1 = n + 1 \bmod n$ ,  $0 = n \bmod n$  and  $-1 = n - 1 \bmod n$  etc. All indices are henceforth understood modulo  $n$ . We choose an arbitrary input point to be  $c_1$ , and the labels of all other input points then follow from the ordering. We still have the freedom to choose which output point is  $r_1$ .

Since  $c_1$  could causally signal all output points, its future antipodal point  $\alpha_1$  must lie between two *adjacent* output points. We can use the freedom of labeling  $r_1$  to choose  $r_1$  to be the output point to the right of  $\alpha_1$ . Then, it follows that  $\alpha_i$  must lie between  $r_{i-1}$  and  $r_i$  for all  $i \in \{1, \dots, n\}$ . As a result, we have  $\alpha_1, r_1, \dots, \alpha_n, r_n$  cyclically ordered (counterclockwise when viewed from future direction) on  $\hat{\Sigma}_2$  (we can choose  $\hat{\Sigma}_2$  to also contain all  $\alpha_i$ 's.).

Similarly, since  $r_j$  can be causally signaled by all  $c_i$ , its past antipodal point  $\beta_j$  must lie between two *adjacent* input points. It is not difficult to see that  $\beta_j$  is forced to lie between  $c_j$  and  $c_{j+1}$  (Figure 1). Therefore, on  $\hat{\Sigma}_1$  (chosen to also contain all  $\beta_j$ 's), we have  $c_1, \beta_1, \dots, c_n, \beta_n$  in cyclic order, whose future light rays to the right and to the left form a coordinate lattice on  $\partial M$ . These light rays are also past light rays to the left and to the right, respectively, from  $\alpha_1, r_1, \dots, \alpha_n, r_n$ .

Figure 1 summarizes the setup for  $n = 3$ . Since we use the flat metric for the conformal boundary  $\partial M$  as usual, one can trust one's intuition in generalizing Figure 1 to general  $n$ .

We also label  $X_j$  and  $Y_i$  associated to  $\beta_j$  and  $\alpha_i$ . That is,

$$X_i = \hat{J}^+[\beta_i] \cap \hat{J}^-[\alpha_1] \cap \cdots \cap \hat{J}^-[\alpha_n],$$

$$Y_i = \hat{J}^-[\alpha_i] \cap \hat{J}^+[\beta_1] \cap \cdots \cap \hat{J}^+[\beta_n],$$

Since  $c_i$  and  $\alpha_i$  are antipodal to each other,  $V_i$  and  $Y_i$  will show up together in following analysis. Similar is true for  $X_j$  and  $W_j$ . For later convenience, we also label spacelike boundaries of  $V_i$ , following [13]. Let  $a_i$  be the common boundary between  $V_i$  and  $X_{i-1}$  and  $b_i$  be the common boundary between  $V_i$  and  $X_{i+1}$ . Let  $e_i$  be the common boundary between  $W_i$  and  $Y_i$  and  $f_i$  be the common boundary between  $W_i$  and  $Y_{i+1}$ . We note that the relative labelling of  $c_i$  and  $\alpha_i$  differs from that in ref. [11] (the  $\alpha_2$  there would be  $\alpha_1$  here).

## 2.2 Causal Anchoring Principle

We recall a crucial observation made in ref. [11]. The Gao-Wald Theorem implies that for a boundary causal domain  $V = \hat{J}^-[p] \cap \hat{J}^+[q]$ , the bulk causal wedge is  $J^+[p] \cap J^-[q]$ . Taking  $c_1$  as an example, both the causal surface of  $V_1$  and that of  $Y_1^c$  lie on the null sheet  $\partial J^+[c_1]$ , equaling its intersection with appropriate bulk Cauchy slices.

Theorems in ref. [15] generalize the Gao-Wald Theorem to homology regions:

$$\mathcal{E}(V) \cap \partial M = \hat{D}(V), \tag{2.2}$$

$$J^\pm[RT(V)] \cap \partial M = \hat{J}^\pm[\partial V]. \tag{2.3}$$

Specifically, null sheets emanating from HRRT surfaces of a causal domain  $V$  are anchored at  $\hat{J}^\pm[\partial V]$  on  $\partial M$ . The same is true for null sheets emanating from causal surfaces, due to the causal wedge-entanglement wedge inclusion relation.

In asymptotically global AdS spacetimes, matter/curvature distorts bulk null sheets  $\mathcal{N}$  relative to their pure AdS counterparts  $\mathcal{N}'$ , but their boundary restrictions  $\mathcal{N} \cap \partial M$  coincide by (2.2) and (2.3). Our proof strategy therefore uses boundary null rays from relevant points to constrain the bulk geometry of entanglement wedges and causal wedges.

## 2.3 Intersections among wedge horizons

Our main proofs rely extensively on geometric relations among null sheets emanating from HRRT surfaces. We therefore summarize some key observations here.

**Lemma 2.1.** *Let  $c_1, c_2$  be two distinct points on a boundary Cauchy slice of the timelike boundary  $\partial M$ . Then the intersection of their boundary causal futures consists of two points,*

$$\hat{J}^+[c_1] \cap \hat{J}^+[c_2] = \{p, q\}.$$

*Consider two bulk causal boundaries  $\mathcal{N}_1$  and  $\mathcal{N}_2$  satisfying*

$$\mathcal{N}_1 \cap \partial M = \hat{J}^+[c_1], \quad \mathcal{N}_2 \cap \partial M = \hat{J}^+[c_2].$$

*Then the intersection*

$$\mathcal{R} := \mathcal{N}_1 \cap \mathcal{N}_2$$

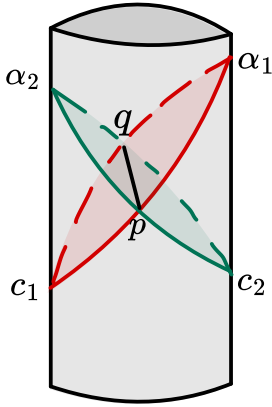


**Figure 2.** Illustration of two relevant null sheets intersecting at a simple ridge.

is a connected, continuous, spacelike, simple (non-self-intersecting) curve with endpoints  $p$  and  $q$  on  $\partial M$ . Moreover,  $\mathcal{R}$  lies entirely in the bulk except at its endpoints. We refer to such an intersection curve as a ridge.

Equivalently, the union  $\mathcal{N}_1 \cup \mathcal{N}_2$  partitions the spacetime into four connected regions.

**Remark 2.2.** Lemma 2.1 obviously applies to  $\mathcal{R} = \partial J^+[c_1] \cap \partial J^+[c_2]$ . In the following, we will apply the lemma to intersections of null sheets emanating from HRRT surfaces that are anchored at  $\partial \hat{J}^+[c_i]$ , for example  $\mathcal{R}_{V_1, V_2} = \partial J^+[RT(V_1)] \cap \partial J^+[RT(V_2)]$ .

That two causal boundaries partition the full spacetime into four regions does not hold in complete generality; counterexamples can be constructed in Minkowski space using compact sets with non-convex boundaries. The assumptions of the lemma exclude such cases.

*Proof.* By assumption,  $\mathcal{N}_i \cap \partial M = \partial \hat{J}^+[c_i]$ , so the two boundary intersection points  $p, q \in \hat{J}^+[c_1] \cap \hat{J}^+[c_2]$  belong to  $\mathcal{R}$ .

Let  $\alpha_1$  be the future antipodal point of  $c_1$ , so that  $\partial \hat{J}^+[c_1] = \partial \hat{J}^+[\alpha_1]$  (see Figure 2 for an illustration). This boundary null curve decomposes into two arcs: one arc  $\gamma_1$  connecting  $p$  to  $\alpha_1$  to  $q$ , and the other arc  $\gamma_2$  connecting  $p$  to  $c_1$  to  $q$ . Both arcs lie on  $\mathcal{N}_1$ . By construction,  $\gamma_1$  lies strictly to the future of  $\mathcal{N}_2$ , while  $\gamma_2$  lies strictly to the past of  $\mathcal{N}_2$ .

As a standard property of causal boundaries,  $\mathcal{N}_1$  is ruled by null geodesic generators, and  $\mathcal{N}_2$  is achronal. Consequently, each null generator of  $\mathcal{N}_1$  can intersect  $\mathcal{N}_2$  at most once: if a generator intersected  $\mathcal{N}_2$  at two distinct points, then the segment between them would lie entirely on one side of  $\mathcal{N}_2$ , allowing the construction of a timelike curve between those two points, contradicting the achronality of  $\mathcal{N}_2$ .

It follows that  $\mathcal{N}_2$  separates  $\mathcal{N}_1$  into exactly two connected components: the portion to the future of  $\mathcal{N}_2$  and the portion to the past of  $\mathcal{N}_2$ . The arcs  $\gamma_1$  and  $\gamma_2$  lie in distinct components of  $\mathcal{N}_1 \setminus (\mathcal{N}_1 \cap \mathcal{N}_2)$ .

Therefore, the intersection  $\mathcal{R} = \mathcal{N}_1 \cap \mathcal{N}_2$  must separate  $\gamma_1$  from  $\gamma_2$  within  $\mathcal{N}_1$ , and hence must contain at least one connected component joining  $p$  to  $q$ . If  $\mathcal{R}$  contained more than one such component, or contained a closed-loop component in the bulk, then some

null generator of  $\mathcal{N}_1$  would necessarily intersect  $\mathcal{N}_2$  more than once, contradicting the single-intersection property established above.

Thus  $\mathcal{R}$  consists of a single connected  $p$ - $q$  curve, which is necessarily spacelike, simple, and entirely bulk-supported except at its endpoints.  $\square$

**Corollary 2.3.** *Let  $c_1, c_2$  and  $\beta$  be three distinct points on a boundary Cauchy slice of the timelike boundary  $\partial M$ . Then the intersection of their boundary causal futures are pairwise nonempty. Consider three bulk causal boundaries  $\mathcal{N}_1, \mathcal{N}_2$  and  $\mathcal{N}_3$  satisfying*

$$\mathcal{N}_1 \cap \partial M = \hat{J}^+[c_1], \quad \mathcal{N}_2 \cap \partial M = \hat{J}^+[c_2], \quad \mathcal{N}_3 \cap \partial M = \hat{J}^+[\beta].$$

*Then the three null sheets intersect at a single point*

$$O = \mathcal{R}_{\mathcal{N}_1, \mathcal{N}_2} \cap \mathcal{R}_{\mathcal{N}_1, \mathcal{N}_3} = \mathcal{R}_{\mathcal{N}_1, \mathcal{N}_2} \cap \mathcal{R}_{\mathcal{N}_2, \mathcal{N}_3} = \mathcal{R}_{\mathcal{N}_1, \mathcal{N}_3} \cap \mathcal{R}_{\mathcal{N}_2, \mathcal{N}_3} = \mathcal{N}_1 \cap \mathcal{N}_2 \cap \mathcal{N}_3,$$

*where  $\mathcal{R}$  with subscripts denote the ridge of intersection between two relevant null sheets.*

*Proof.* By Lemma 2.1, each pair  $\mathcal{N}_i, \mathcal{N}_j$  intersects along a unique ridge

$$\mathcal{R}_{\mathcal{N}_i, \mathcal{N}_j} := \mathcal{N}_i \cap \mathcal{N}_j,$$

which is a continuous, simple, spacelike curve with endpoints on  $\partial M$ . In particular,  $\mathcal{R}_{\mathcal{N}_1, \mathcal{N}_2}$  is nonempty.

**Step 0:**  $\mathcal{R}_{\mathcal{N}_1, \mathcal{N}_2} \cap \mathcal{N}_3 \neq \emptyset$ . This follows from the boundary ordering: the endpoints of  $\mathcal{R}_{\mathcal{N}_1, \mathcal{N}_2}$  on  $\partial M$  lie in different components of  $\partial M \setminus \hat{J}^+[\beta]$ , so the connected curve  $\mathcal{R}_{\mathcal{N}_1, \mathcal{N}_2}$  must cross  $\mathcal{N}_3$ .

**Step 1:  $\mathcal{R}_{\mathcal{N}_1, \mathcal{N}_2} \cap \mathcal{N}_3$  cannot contain a curve segment.** Suppose for contradiction that  $\mathcal{R}_{\mathcal{N}_1, \mathcal{N}_2} \cap \mathcal{N}_3$  contains a nontrivial segment  $I$ . Then  $I \subset \mathcal{N}_1 \cap \mathcal{N}_2 \cap \mathcal{N}_3$ . Assume there exists a point  $x \in I$  at which all three hypersurfaces  $\mathcal{N}_1, \mathcal{N}_2, \mathcal{N}_3$  admit tangent planes and hence have well-defined null generator directions.

Because  $I$  is spacelike (as a subcurve of the ridge  $\mathcal{R}_{\mathcal{N}_1, \mathcal{N}_2}$ ), its normal plane  $N_x I$  has Lorentzian signature  $(-1, 1)$  and therefore contains exactly two null directions. For a differentiable null hypersurface  $\mathcal{N}_i$  containing  $I$ , its null generator at  $x$  must be orthogonal to  $T_x I$ , hence must lie in  $N_x I$  and coincide with one of these two null directions. Therefore, among the three null sheets  $\mathcal{N}_1, \mathcal{N}_2, \mathcal{N}_3$  through  $x$ , at least two have the same null generator direction at  $x$ .

Since those two hypersurfaces both contain the same spacelike segment  $I$  through  $x$  and share the same null generator direction at  $x$ , they coincide in a neighborhood of  $x$  as ruled null hypersurfaces. This contradicts the distinct boundary anchoring data  $\mathcal{N}_1 \cap \partial M = \hat{J}^+[c_1], \mathcal{N}_2 \cap \partial M = \hat{J}^+[c_2], \mathcal{N}_3 \cap \partial M = \hat{J}^+[\beta]$  for distinct boundary points. Hence  $\mathcal{R}_{\mathcal{N}_1, \mathcal{N}_2} \cap \mathcal{N}_3$  contains no nontrivial segment.

**Step 2:  $\mathcal{R}_{\mathcal{N}_1, \mathcal{N}_2} \cap \mathcal{N}_3$  contains at most one point.** By Step 1,  $\mathcal{R}_{\mathcal{N}_1, \mathcal{N}_2} \cap \mathcal{N}_3$  is a discrete set of points. Assume for contradiction that it contains two distinct points  $O_1 \neq O_2$ . Since  $\mathcal{N}_3$  is an achronal causal boundary, it locally separates  $\bar{M}$  into a future side and a past side.

If  $\mathcal{R}_{\mathcal{N}_1, \mathcal{N}_2} \cap \mathcal{N}_3$  contains two distinct points  $O_1 \neq O_2$ , then along the connected spacelike curve  $\mathcal{R}_{\mathcal{N}_1, \mathcal{N}_2}$  there exists an open segment whose interior lies entirely on one side of  $\mathcal{N}_3$ . This segment determines a “hole” between  $\mathcal{R}_{\mathcal{N}_1, \mathcal{N}_2}$  and  $\mathcal{N}_3$ .

The ridge  $\mathcal{R}_{\mathcal{N}_1, \mathcal{N}_2}$  is contained in both null hypersurfaces  $\mathcal{N}_1$  and  $\mathcal{N}_2$ . At most one of these null hypersurfaces can contain the hole entirely. Since  $\mathcal{N}_1$  and  $\mathcal{N}_2$  are distinct causal boundaries, the other null hypersurface must intersect  $\mathcal{N}_3$  on both sides of the hole, and hence must enter and leave one side of  $\mathcal{N}_3$ .

This contradicts Lemma 2.1 applied to the corresponding pair  $(\mathcal{N}_1, \mathcal{N}_3)$  or  $(\mathcal{N}_2, \mathcal{N}_3)$ , which guarantees that two such causal boundaries separate the spacetime into four connected components. Hence  $\mathcal{R}_{\mathcal{N}_1, \mathcal{N}_2} \cap \mathcal{N}_3$  contains at most one point.

**Step 3: Identification of the triple intersection point.** Let  $O$  denote the unique point in  $\mathcal{R}_{\mathcal{N}_1, \mathcal{N}_2} \cap \mathcal{N}_3$ . Then  $O \in \mathcal{N}_1 \cap \mathcal{N}_2 \cap \mathcal{N}_3$ , hence  $O$  lies on each pairwise ridge. Therefore

$$O = \mathcal{R}_{\mathcal{N}_1, \mathcal{N}_2} \cap \mathcal{R}_{\mathcal{N}_1, \mathcal{N}_3} = \mathcal{R}_{\mathcal{N}_1, \mathcal{N}_2} \cap \mathcal{R}_{\mathcal{N}_2, \mathcal{N}_3} = \mathcal{R}_{\mathcal{N}_1, \mathcal{N}_3} \cap \mathcal{R}_{\mathcal{N}_2, \mathcal{N}_3} = \mathcal{N}_1 \cap \mathcal{N}_2 \cap \mathcal{N}_3,$$

as claimed.  $\square$

**Definition 2.4** (Geometric ordering of ridges). *Let  $c_1, c_2$  and  $\beta_1, \beta_2$  be four distinct points on a boundary Cauchy slice of the timelike boundary  $\partial M$ . Let  $\mathcal{N}_1 = \partial J^+[\mathcal{U}_1]$  and  $\mathcal{N}_2 = \partial J^+[\mathcal{U}_2]$  be two bulk future causal boundaries satisfying*

$$\mathcal{N}_1 \cap \partial M = \hat{J}^+[c_1], \quad \mathcal{N}_2 \cap \partial M = \hat{J}^+[c_2],$$

*and let  $\mathcal{N}_3 = \partial J^-[\mathcal{U}_3]$  and  $\mathcal{N}_4 = \partial J^-[\mathcal{U}_4]$  be two bulk past causal boundaries satisfying*

$$\mathcal{N}_3 \cap \partial M = \hat{J}^+[\beta_1], \quad \mathcal{N}_4 \cap \partial M = \hat{J}^+[\beta_2].$$

*Denote the ridges by*

$$\mathcal{R}_{\mathcal{U}_1, \mathcal{U}_2} := \mathcal{N}_1 \cap \mathcal{N}_2, \quad \mathcal{R}_{\mathcal{U}_3, \mathcal{U}_4} := \mathcal{N}_3 \cap \mathcal{N}_4.$$

*We say that the ridge  $\mathcal{R}_{\mathcal{U}_1, \mathcal{U}_2}$  lies below  $\mathcal{R}_{\mathcal{U}_3, \mathcal{U}_4}$  if*

$$J^+[\mathcal{U}_1] \cap J^+[\mathcal{U}_2] \cap J^-[\mathcal{U}_3] \cap J^-[\mathcal{U}_4] \neq \emptyset.$$

*Otherwise, we say that  $\mathcal{R}_{\mathcal{U}_1, \mathcal{U}_2}$  lies above  $\mathcal{R}_{\mathcal{U}_3, \mathcal{U}_4}$ , i.e.*

$$J^+[\mathcal{U}_1] \cap J^+[\mathcal{U}_2] \cap J^-[\mathcal{U}_3] \cap J^-[\mathcal{U}_4] = \emptyset.$$

**Remark 2.5.** Definition 2.4 is a convenient shorthand for the causal relation between the two ridges. In the present framework, Lemma 2.1 implies that each ridge is a unique simple curve with fixed boundary endpoints, and Corollary 2.3 controls triple intersections of causal boundaries. Together, these results exclude pathological configurations discussed in our previous work [11], such as:

- the two ridges intertwining (e.g. one “spiraling” around the other);
- the two ridges intersecting at more than one point.

Indeed, any such configuration would force repeated entering/leaving behavior among causal boundaries, contradicting Lemma 2.1.

## 2.4 Characterization of connected entanglement wedges

Lastly, we recall some basic facts about a multipartite entanglement wedge being connected or multipartite mutual information being nonzero. We assume familiarity with these concepts as presented in Refs. [16, 17].

**Lemma 2.6.** *Consider a union of disjoint subsets  $V_1 \cup \dots \cup V_n$  and its causal complement  $X_1 \cup \dots \cup X_n = (V_1 \cup \dots \cup V_n)^c$ . The following are equivalent:*

1.  $\mathcal{E}(V_1 \cup \dots \cup V_n)$  is connected.
2. For any nontrivial (nonempty) bipartition of  $V_1 \cup \dots \cup V_n = A \cup B$ , the mutual information  $I(A : B) > 0$ .
3.  $\mathcal{E}(X_1 \cup \dots \cup X_n)$  is fully disconnected<sup>1</sup>.

Further, one has

**Lemma 2.7.** *If  $\mathcal{E}(X_1 \cup \dots \cup X_n)$  is fully disconnected, i.e.  $\mathcal{E}(X_1 \cup \dots \cup X_n) = \mathcal{E}(X_1) \cup \dots \cup \mathcal{E}(X_n)$ , or equivalently*

$$S(X_1 \cup \dots \cup X_n) = S(X_1) + \dots + S(X_n)$$

*in terms of entropy. Then any subset  $A \subseteq X_1 \cup \dots \cup X_n$  also has fully disconnected entanglement wedge, i.e.*

$$\mathcal{E}(A) = \bigcup_{X_i \in A} \mathcal{E}(X_i)$$

*or in terms of entropy,*

$$S(A) = \sum_{X_i \in A} S(X_i)$$

*Proof.* If  $\mathcal{E}(A)$  is connected or partially connected, then its HRRT surfaces are composed of a union of surfaces with strictly smaller total area than  $\bigcup_{X_i \in A} RT(X_i)$ . Combining with  $\bigcup_{X_j \notin A} RT(X_j)$ , this gives a candidate HRRT surface for  $X_1 \cup \dots \cup X_n = A \cup A^c$  with strictly smaller area than  $\bigcup_i RT(X_i)$ . This would contradict the condition that  $\mathcal{E}(X_1 \cup \dots \cup X_n)$  is fully disconnected.  $\square$

**Lemma 2.8.** *Consider a union of disjoint subsets  $V_1 \cup \dots \cup V_n$ . If the entanglement wedge of any pair is connected, or equivalently,*

$$I(V_i : V_j) > 0, \forall i \neq j$$

*then,  $\mathcal{E}(V_1 \cup \dots \cup V_n)$  is connected.*

*Proof.* By Lemma 2.6, to show that  $\mathcal{E}(V_1 \cup \dots \cup V_n)$  is connected it suffices to show that  $I(A : B) > 0$  for every nontrivial bipartition  $V_1 \cup \dots \cup V_n = A \cup B$ . Then the Lemma follows directly from the monotonicity of mutual information or strong subadditivity: for any  $V_i \subseteq A, V_j \subseteq B$  one has  $I(A : B) \geq I(V_i : V_j) > 0$ .  $\square$

<sup>1</sup>Since there are partially connected cases when  $n > 2$ , we use fully disconnected to refer to the case of  $\mathcal{E}(X_1 \cup \dots \cup X_n) = \mathcal{E}(X_1) \cup \dots \cup \mathcal{E}(X_n)$

**Remark 2.9.** If one only assumes that  $\mathcal{E}(V_1 \cup \dots \cup V_n)$  is connected, the entanglement wedge of any pair could be disconnected. Simple examples can be constructed in pure  $AdS_3$ .

In light of the  $\Gamma_{2 \rightarrow \text{all}}$  graph introduced by ref. [13], we can introduce a mutual information graph  $\tilde{\Gamma}$  whose vertices  $1, 2, \dots, n$  represent the input regions  $V_i$ 's and whose edge  $i - j$  represents  $I(V_i : V_j) \sim O(1/G_N)$ . The following lemma could make the interpretation of Theorem 1.2 of ref. [13] more transparent.

**Lemma 2.10.** If the mutual information graph  $\tilde{\Gamma}$  is connected, then  $\mathcal{E}(V_1 \cup \dots \cup V_n)$  is connected.

A special case is that pairwise mutual information  $I(V_i : V_j) > 0, \forall i \neq j$ .

*Proof.* For a set  $V_1 \cup \dots \cup V_n$  to have connected entanglement wedges, any nontrivial (nonempty) bipartition of  $V_1 \cup \dots \cup V_n = A \cup B$  should have strictly positive mutual information, i.e.

$$I(A : B) > 0.$$

If  $\tilde{\Gamma}$  is connected, then for any bipartition  $V_1 \cup \dots \cup V_n = A \cup B$ , there would exist  $V_i \in A$  and  $V_j \in B$  such that  $I(V_i : V_j) > 0$ . Then applying inductively the monotonicity of mutual information  $I(V_1 : V_2 \cup V_3) \geq I(V_1 : V_2)$ , one would have

$$I(A : B) \geq I(V_i : V_j) > 0.$$

□

In fact, as shown in Ref. [18], one can give a complete information theoretical characterization of connected multipartite entanglement wedges using multipartite mutual information

$$I_n(V_1 : \dots : V_n) = \sum_{k=1}^n (-1)^{k-1} \sum_{i_1 < \dots < i_k} S(V_{i_1} \cup \dots \cup V_{i_k}). \quad (2.4)$$

For example, the monogamy of mutual information (MMI)

$$S(V_1) + S(V_2) + S(V_3) + S(V_1 \cup V_2 \cup V_3) \geq S(V_1 \cup V_2) + S(V_1 \cup V_3) + S(V_2 \cup V_3) \quad (2.5)$$

which holds for holographic states but not general quantum states can be recast as

$$-I_3(V_1 \cup V_2 \cup V_3) \geq 0.$$

We document here a theorem of ref. [18] for completeness.

**Theorem 2.11.** The multipartite information of  $n$  disjoint subsystems  $V_i$  in a generic configuration<sup>2</sup> is nonvanishing  $I_n(V_1 : \dots : V_n) \neq 0$  if and only if the joint entanglement wedge of  $\mathcal{E}(V_1 \cup \dots \cup V_n)$  is connected.

<sup>2</sup>By generic configuration, they exclude phase transition cases when multiple extremal surfaces exchange dominance

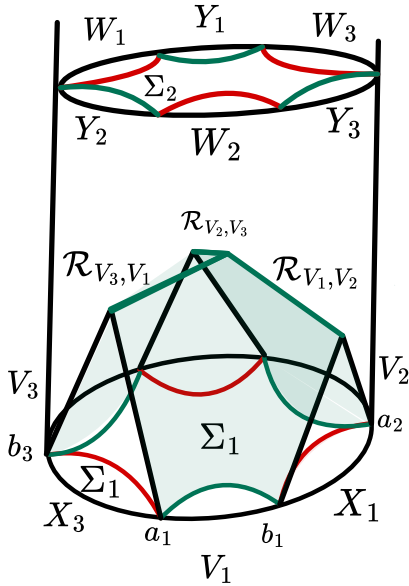


**Figure 3.** Illustration of the surface  $\mathcal{Z}_{in}$  formed by future null sheets emanating from  $RT(V_i)$  for  $n = 3$ . Green curves in  $\Sigma_1$  and  $\Sigma_2$  lie on  $\partial J^+[\mathcal{E}(V_i)]$  while red curves in  $\Sigma_1$  and  $\Sigma_2$  lie on  $\partial J^-[\mathcal{E}(W_j)]$ . The ridges  $\mathcal{R}_{V_i, V_{i+1}} = \partial J^+[\mathcal{E}(V_i)] \cap \partial J^+[\mathcal{E}(V_{i+1})]$  are labeled explicitly. Note that  $n + 1 = 1$  because of the  $S^1$  topology.

### 3 Generalizing the n-to-n Connected Wedge Theorem

#### 3.1 An improvement of the n-to-n Connected Wedge Theorem

Let us start with giving a slightly different proof of the  $n$ -to- $n$  Connected Wedge Theorem, which also reveals that the necessary condition of Theorem 1.2 can be further weakened, as stated in Theorem 1.3.

For the purpose of explanation, let us pick  $\Sigma_1$  to be a bulk Cauchy slice bounded by  $\hat{\Sigma}_1$  and containing relevant HRRT surfaces<sup>3</sup>. Similarly, let  $\Sigma_2$  be a bulk Cauchy slice bounded by  $\hat{\Sigma}_2$  that contains relevant HRRT surfaces.

We consider the geometric surface  $\mathcal{Z}_{in} := \partial J^+[\mathcal{E}(V_1 \cup \dots \cup V_n)]$ . In the fully disconnected case, the surface  $\mathcal{Z}_{in}$  is formed by the union of all future-pointing null sheets  $\mathcal{N}_{V_i} = \partial J^+[\mathcal{E}(V_i)]$  that emanate from  $RT(V_i)$ , truncated at their mutual intersections (see Figure 3 for an illustration with  $n = 3$ ). The surface  $\mathcal{Z}_{in}$  is therefore made up of null sheets intersecting at a net of vertices and (subsets of) ridges. Noting that  $\mathcal{N}_{V_i}$  is also the future horizon of  $\mathcal{E}(V_i^c)$ <sup>4</sup>, this surface  $\mathcal{Z}_{in}$  is also the future boundary of the compact set  $\cap_{i=1}^n \mathcal{E}(V_i^c)$ . Also note that  $\mathcal{Z}_{in}$  and  $\Sigma_1$  bound a compact subset of  $\overline{M} = M \cup \partial M$ , which will be denoted by  $\mathcal{Z}_B$ .

<sup>3</sup>This is always possible because HRRT surfaces of disjoint spacelike-separated boundary regions can be minimal on the same Cauchy slice [19].

<sup>4</sup>Recall that superscript  $c$  indicates causal complements

We also consider past-pointing null sheets  $\mathcal{N}_{W_j} = \partial J^-[RT(W_j)]$  that emanate from  $RT(W_j)$ 's. Note that  $\mathcal{N}_{W_j}$  is also the past horizon of  $\mathcal{E}(W_j^c)$ . By the causal anchoring principle,  $\mathcal{N}_{V_i} \cap \partial M$  and  $\mathcal{N}_{W_i} \cap \partial M$ , are just light rays emitted from  $c_i$  and  $r_j$  (or  $\beta_j$ ), respectively.

Due to cyclic boundary ordering  $V_1, X_1, \dots, V_n, X_n$  (and similarly for the outputs), the null sheet  $\mathcal{N}_{W_i}$ , which is anchored at the spatial boundaries  $b_i$  and  $a_{i+1}$  of  $X_i$ , is topologically constrained to intersect the surface  $\mathcal{Z}_{in}$ . We assert that this intersection  $\mathcal{C}_i$ , is a simple curve on  $\mathcal{Z}_{in}$  with endpoints precisely at  $b_i$  and  $a_{i+1}$ . The argument proceeds in two steps. First, within the bulk region  $\mathcal{Z}_B$  bounded by  $\mathcal{Z}_{in}$  and the Cauchy slice  $\Sigma_1$ , the intersection  $\mathcal{C}_i$  is homotopic to  $\mathcal{N}_{W_i} \cap \Sigma_1$ , which is itself homotopic to the HRRT surface  $RT(X_i)$  within  $\Sigma_1$ . Second, Lemma 2.1 excludes the possibility that  $\mathcal{C}_i$  contain homotopically trivial closed loops:  $\mathcal{N}_{W_j} \cap \mathcal{N}_{V_i}$  is a simple ridge in  $\mathcal{N}_{V_i}$  and  $\mathcal{Z}_{in}$  is made up of intersecting null sheets  $\mathcal{N}_{V_i}$ 's. This concludes that  $\mathcal{C}_i$  is a simple curve without disconnected components. A simple illustration for the  $n = 3$  case is provided in Figure 4(a). Moreover, each curve  $\mathcal{C}_i$  must have segments in at least the adjacent null sheets  $\mathcal{N}_{V_i}$  and  $\mathcal{N}_{V_{i+1}}$ , though it may also cross other sheets that constitute  $\mathcal{Z}_{in}$ .

We now prove that if all curves  $\mathcal{C}_i$  are distinct, the entanglement wedge cannot decompose as a disjoint union  $\mathcal{E}(V_1) \cup \dots \cup \mathcal{E}(V_n)$ . The proof constructs a specific geometric comparison on the null surface  $\mathcal{Z}_{in}$ , following a strategy analogous to the original CWT proof [8].

The key observation is that the set of  $\bigcup_{i=1}^n \mathcal{C}_i$  are homologous to  $\bigcup_{i=1}^n RT(V_i)$  on  $\mathcal{Z}_{in}$ . Specifically, each  $\mathcal{N}_{V_i}$  component of  $\mathcal{Z}_{in}$  is bounded by the curve  $RT(V_i)$  and ridge segments formed at intersection of  $\mathcal{N}_{V_i}$  with adjacent null sheets, e.g.  $\mathcal{N}_{V_{i-1}}$  and  $\mathcal{N}_{V_{i+1}}$  and potentially other null sheets. This structure forces the adjacent curves  $\mathcal{C}_{i-1}$  and  $\mathcal{C}_i$  to exit  $\mathcal{N}_{V_i}$  by intersecting these ridge segments. Consequently, within each null sheet  $\mathcal{N}_{V_i}$ , the curve  $RT(V_i)$  is homologous to a composite curve  $\tilde{\gamma}_i$ . This curve  $\tilde{\gamma}_i$  is formed by joining the segments of  $\mathcal{C}_{i-1}$  and  $\mathcal{C}_i$  with the relevant ridge segments between their exit points, possibly also other  $\mathcal{C}_k$  ( $k \neq i, i-1$ ) that enters  $\mathcal{N}_{V_i}$ . For example, in the  $n = 3$  case illustrated in Figure 4, the curve  $\tilde{\gamma}_1$  would be the union of the segment  $a_1 - d_3$  (from  $\mathcal{C}_0 = \mathcal{C}_3$ ),  $b_1 - d_1$  (from  $\mathcal{C}_1$ ), and the ridge segments  $O - d_3$  and  $O - d_1$ .

An area comparison follows from the focusing property (non-positive null expansion,  $\theta \leq 0$ ) on null sheets emanating from extremal surfaces. Moving along the sheets away from  $RT(V_i)$ , this implies:

$$|\tilde{\gamma}_i| \leq |RT(V_i)|. \quad (3.1)$$

Furthermore, by construction, the original curves  $\bigcup_{i=1}^n \mathcal{C}_i$  are contained within this new set  $\bigcup_{i=1}^n \tilde{\gamma}_i$ :

$$\bigcup_{i=1}^n \mathcal{C}_i \subseteq \bigcup_{i=1}^n \tilde{\gamma}_i, \quad (3.2)$$

where the inclusion is strict if any ridge segment is included in  $\tilde{\gamma}_i$ .

On  $\mathcal{N}_{W_i}$ , pushing  $\mathcal{C}_i$  along past null generators until one encounters  $\Sigma_1$ , one gets

$$|\mathcal{C}_i| \geq |\mathcal{N}_{W_i} \cap \Sigma_1| \geq |RT(X_i)|. \quad (3.3)$$

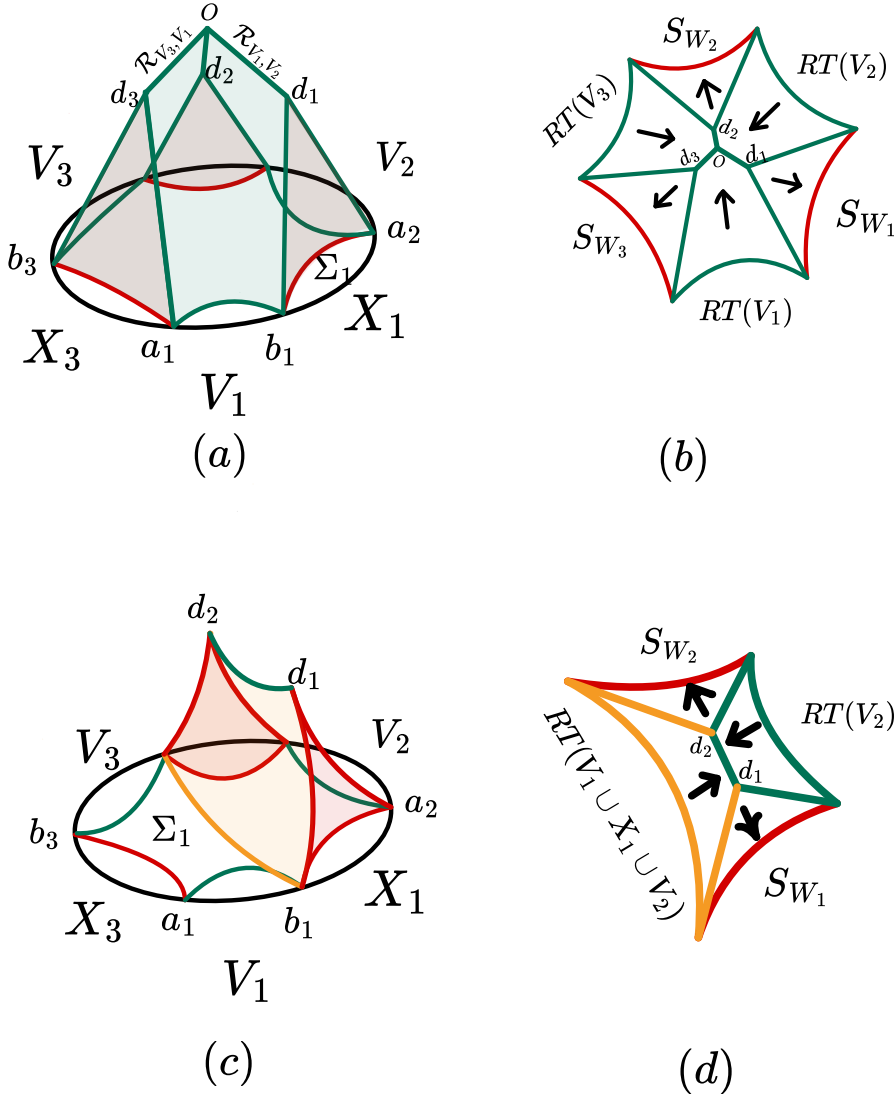


**Figure 4.** Illustration of focusing calculation when  $n=3$ . Panel (a) shows the geometric structure  $\mathcal{Z}_{in}$  cut by  $\partial J^-[E(W_i)]$  (compare with Figure 3), where future null sheets emanating from  $RT(V_i)$  are shown in green and past null sheets emanating from  $RT(W_i)$  are shown in red. The curves  $C_i = \partial J^-[E(W_i)] \cap \mathcal{Z}_{in}$  is shown as  $b_i - d_i - a_{i+1}$  (counting modulo  $n$ ). Panel (b) show the  $\mathcal{Z}_{in}$  in a flattened fashion where  $S_{W_i}$  is the intersection of null sheet  $\partial J^-[E(W_i)]$  with  $\Sigma_1$ , i.e.  $S_{W_i} = \partial J^-[E(W_i)] \cap \Sigma_1$ . Arrows indicate the direction along which null expansion  $\theta$  decreases. Panels (c) and (d) are similar to panels (a) and (b) but for partially connected scenarios.

because  $\theta \leq 0$  along the past direction on  $\mathcal{N}_{W_i}$ . We also used that  $RT(X_i)$  is minimal among all surfaces on  $\Sigma_1$  that homologous to  $X_i$ , by our choice of  $\Sigma_1$ . Combining (3.1), (3.2) and (3.3), one gets

$$\sum_i |RT(V_i)| \geq \sum_i |RT(X_i)|, \quad (3.4)$$

where the inequality is strict if  $\cup \tilde{\gamma}_i$  contains any ridge segment. In the above calculation we neglect additional endpoints of null generators due to focusing inside  $\mathcal{N}_{V_i}$  or  $\mathcal{N}_{W_j}$  (see ref. [8] or ref. [11] for details). Including these only makes the inequality stronger. Equation (3.4) implies that  $\mathcal{E}(V_1 \cup \dots \cup V_n)$  cannot be fully disconnected.

We next address partially connected configurations. Recall that  $Z_{in} = \partial J^+[\mathcal{E}(V_1 \cup \dots \cup V_n)]$  by definition; in partially connected phases this surface is generated by null sheets from HRRT surfaces of enlarged input regions. These enlarged input regions take the form  $V_k \cup X_k \cup \dots \cup V_{k+l}$  and remain separated by a subset of the original complement regions  $X_j$ 's. A key consequence of entanglement wedge nesting is that this new surface  $\mathcal{Z}_{in}$  lies inside the compact region  $\mathcal{Z}_B$ . In other words, this new  $\mathcal{Z}_{in}$  lies nowhere to the future of the original  $\mathcal{Z}_{in}$  formed solely from  $\mathcal{N}_{V_i}$ .

This inclusion relation ensures that the new intersection curves  $\mathcal{C}_j = \mathcal{N}_{W_j} \cap \mathcal{Z}_{in}$  (defined for the set of  $j$  with  $X_j$  remaining as complements of the enlarged input regions) remain simple and distinct from one another. With this geometric structure in place, one can perform a length/area comparison analogous to the previous connected case. This calculation leads to the conclusion that the length of HRRT surfaces for the enlarged input regions must exceed the sum  $\sum |RT(X_j)|$ , where the sum runs only over the  $X_j$  appearing as complements. This inequality presents a contradiction, thereby proving that  $\mathcal{E}(V_1 \cup \dots \cup V_n)$  cannot be in a partially connected state.

The preceding geometric proof establishes a general criterion: any condition that ensures the intersection curves  $\mathcal{C}_i$  are distinct on  $\mathcal{Z}_{in}$  is sufficient to conclude that  $\mathcal{E}(V_1 \cup \dots \cup V_n)$  is connected. This criterion can be formulated as the requirement that for all distinct output pairs  $i \neq j$ ,

$$[\bigcap_{k=1}^n \mathcal{E}(V_k^c)] \cap [\mathcal{E}(W_i^c) \cap \mathcal{E}(W_j^c)] = \emptyset, \quad (3.5)$$

or rephrased in pairwise terms,

$$\forall i \neq j, \exists k \neq l \text{ such that } \mathcal{E}(V_k^c) \cap \mathcal{E}(V_l^c) \cap \mathcal{E}(W_i^c) \cap \mathcal{E}(W_j^c) = \emptyset. \quad (3.6)$$

In words, for each output pair  $(i, j)$  there exists an input pair  $(k, l)$  such that the ridge  $\mathcal{R}_{V_k, V_l}$  lies below the ridge  $\mathcal{R}_{W_i, W_j}$ .

A particularly useful, more explicit condition that implies (3.6) is the following:

$$\exists k \neq l \text{ such that } J^+[\mathcal{E}(V_k)] \cap J^+[\mathcal{E}(V_l)] \cap \bigcap_{i=1}^n J^-[\mathcal{E}(W_i)] \neq \emptyset \quad (3.7)$$

In words, the ridge  $\mathcal{R}_{V_k, V_l}$  lies below all ridges  $\cup_{i \neq j} \mathcal{R}_{W_i, W_j}$ .

Condition (3.7) is strictly weaker than the original connected graph  $\Gamma_{2 \rightarrow \text{all}}$  condition of ref. [13]. In short terms, we only require the existence of one instance of  $2 \rightarrow \text{all}$  while connected graph  $\Gamma_{2 \rightarrow \text{all}}$  requires at least  $n - 1$  such instances.

### 3.2 Consequences of connected entanglement wedges

We now discuss consequences of  $\mathcal{E}(V_1 \cup \dots \cup V_n)$  being connected. When  $\mathcal{E}(V_1 \cup \dots \cup V_n)$  is connected, it is natural to work with the future horizon of  $\mathcal{E}(V_1 \cup \dots \cup V_n)$ , which is formed by future null sheets  $\mathcal{N}_{X_i}$  emanating from  $RT(X_i)$ . Accordingly, we compare these sheets with past-pointing null sheets emanating from  $RT(Y_i)$ , and we formulate the consequences below in terms of *ridges* entering  $\mathcal{E}(V_1 \cup \dots \cup V_n)$ .

#### 3.2.1 Consequence from a connected–disconnected area comparison

We first derive a necessary geometric consequence of  $\mathcal{E}(V_1 \cup \dots \cup V_n)$  being connected by a contradiction argument comparing the connected and fully disconnected phases:

$$\exists k \neq l \text{ such that } \mathcal{E}(Y_k^c) \cap \mathcal{E}(Y_l^c) \cap \mathcal{E}(V_1 \cup \dots \cup V_n) \neq \emptyset. \quad (3.8)$$

Equivalently, there exists a ridge

$$\mathcal{R}_{Y_k, Y_l} := \partial J^-[RT(Y_k)] \cap \partial J^-[RT(Y_l)]$$

that *enters*  $\mathcal{E}(V_1 \cup \dots \cup V_n)$ , or, in the ridge-ordering language, lies below all ridges  $\mathcal{R}_{X_i, X_j} := \partial J^+[RT(X_i)] \cap \partial J^+[RT(X_j)]$  for all  $i \neq j$  (since  $\mathcal{E}(V_1 \cup \dots \cup V_n) = \bigcap_{i=1}^n \mathcal{E}(X_i^c)$ ).

**(Optional) scattering interpretation.** If we additionally assume  $\mathcal{E}(W_1 \cup \dots \cup W_n)$  is connected, then by Lemma 2.6 this is equivalent to  $\mathcal{E}(Y_1 \cup \dots \cup Y_n)$  being fully disconnected. In that case, for any pair  $k \neq l$ ,  $\mathcal{E}(Y_k \cup Y_l)$  is disconnected (Lemma 2.7), i.e. the two components of  $(Y_k \cup Y_l)^c$  have connected entanglement wedges. We refer to these two components as *modified output regions*:

$$\begin{aligned} \tilde{W}_k &= W_k \cup Y_{k+1} \cup \dots \cup W_{l-1}, \\ \tilde{W}_l &= W_l \cup Y_{l+1} \cup \dots \cup W_{k-1}, \end{aligned} \quad (3.9)$$

with indices understood modulo  $n$ . We define the corresponding *modified output points*  $\tilde{r}_k, \tilde{r}_l$  by

$$\tilde{W}_k = \hat{J}^-(\tilde{r}_k) \cap \hat{J}^+(c_k) \cap \hat{J}^+(c_l), \quad (3.10)$$

$$\tilde{W}_l = \hat{J}^-(\tilde{r}_l) \cap \hat{J}^+(c_k) \cap \hat{J}^+(c_l), \quad (3.11)$$

where  $c_k, c_l$  are the corresponding input points. See Figure 6(a) for an illustration when  $n = 3$ .

With these definitions, (3.8) can be rephrased as

$$\exists k \neq l \text{ such that } \mathcal{E}(V_1 \cup \dots \cup V_n) \cap \mathcal{E}(\tilde{W}_k \cup \tilde{W}_l) \neq \emptyset. \quad (3.12)$$

Or in pairwise terms,

$$\exists k \neq l \text{ such that } \forall i \neq j, \quad \mathcal{E}(\tilde{V}_i \cup \tilde{V}_j) \cap \mathcal{E}(\tilde{W}_k \cup \tilde{W}_l) \neq \emptyset, \quad (3.13)$$

where  $\tilde{V}_i \cup \tilde{V}_j = (X_i \cup X_j)^c$ .

**Proof of (3.8).** We argue by contradiction. Assume that for all  $k \neq l$ ,

$$\mathcal{E}(Y_k^c) \cap \mathcal{E}(Y_l^c) \cap \mathcal{E}(V_1 \cup \dots \cup V_n) = \emptyset,$$

equivalently every ridge  $\mathcal{R}_{Y_k, Y_l}$  lies strictly above  $\mathcal{E}(V_1 \cup \dots \cup V_n)$ . Let  $\mathcal{Z}_{in}$  denote the future horizon of  $\mathcal{E}(V_1 \cup \dots \cup V_n)$ , i.e. the surface formed by future null sheets emanating from the  $RT(X_i)$  up to their intersections. As in Section 3.1, each past horizon  $\mathcal{N}_{Y_k} := \partial J^-[E(Y_k)]$  intersects  $\mathcal{Z}_{in}$  in a simple curve  $\mathcal{C}_k$  with endpoints  $a_k, b_k$ . If all ridges lie above  $\mathcal{Z}_{in}$ , then these curves are all distinct: intersections  $\mathcal{C}_k \cap \mathcal{C}_l$  would correspond to where the ridge  $\mathcal{N}_{Y_k} \cap \mathcal{N}_{Y_l}$  enters/leaves  $\mathcal{E}(V_1 \cup \dots \cup V_n)$ <sup>5</sup>. In this situation one repeats the focusing calculation of Section 3.1 to obtain

$$|RT(X_i)| \geq |RT(V_i)|, \quad (3.14)$$

contradicting that  $\mathcal{E}(V_1 \cup \dots \cup V_n)$  is connected. This establishes (3.8). See Figure 5(a–b) for an illustration when  $n = 3$ .

### 3.2.2 Consequences from pairwise consideration

We now derive further necessary geometric consequences of  $\mathcal{E}(V_1 \cup \dots \cup V_n)$  being connected by exploiting pairwise disconnectedness of  $\mathcal{E}(X_i \cup X_j)$  (equivalently  $I(X_i : X_j) = 0$ ). For  $n = 3$  this pairwise condition admits a direct “partially connected phase” interpretation (see Remark 3.1); for general  $n$  it serves as the *base layer* input of a layered reduction on the boundary lattice.

**Remark 3.1.** For  $n = 3$ ,  $\mathcal{E}(V_1 \cup V_2 \cup V_3)$  is connected if and only if the following hold:

- $\sum_{i=1}^3 |RT(X_i)| \leq \sum_{i=1}^3 |RT(V_i)|$ ,
- $I(X_i : X_j) = 0$  for all pairs  $i \neq j$ .

The second item is equivalent to excluding the partially connected phases for  $n = 3$ , so the two items above are complete in this sense. For  $n > 3$ , the role of the pairwise condition is different: it is the starting point of a layered reduction that ultimately produces an entering ridge at the top layer (Section 3.2.3).

**Illustration for  $n = 3$  (one step of the mechanism).** Consider the boundary causal diamond

$$\hat{J}^+[\beta_1] \cap \hat{J}^+[\beta_2] \cap \hat{J}^-[\alpha_1] \cap \hat{J}^-[\alpha_3],$$

which we denote by  $\tilde{Y}_1$  (see Figure 1)<sup>6</sup>. The past-pointing null sheet emanating from  $RT(\tilde{Y}_1)$  intersects  $\Sigma_1$  along a curve homologous to  $RT(X_1 \cup V_2 \cup X_2)$ .

Suppose that the ridge

$$\mathcal{R}_{\tilde{Y}_1, Y_2} := \partial J^-[RT(\tilde{Y}_1)] \cap \partial J^-[RT(Y_2)]$$

---

<sup>5</sup>One can show any ridge enters and leaves  $\mathcal{Z}_{in}$  at most once using Lemma 2.1 and Corollary 2.3.

<sup>6</sup>This is analogous to the 2-to- $(n - 1)$  scattering region discussed in Ref. [13], where it is shown to be nonempty.

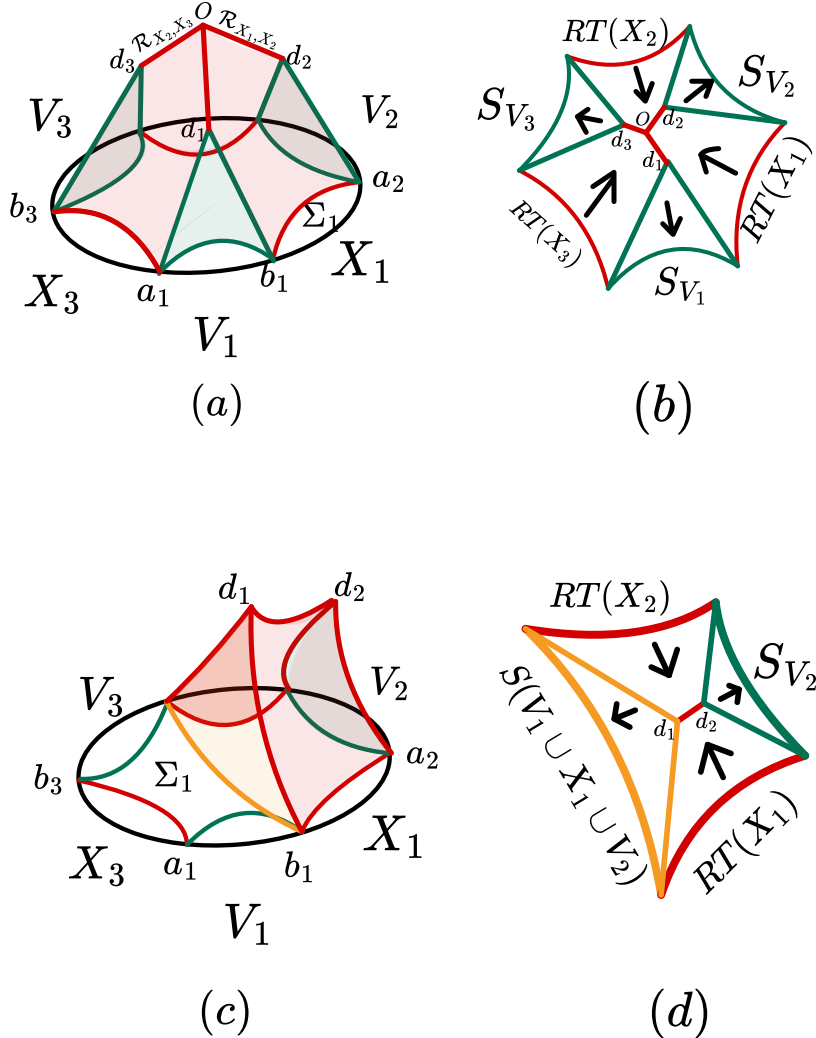
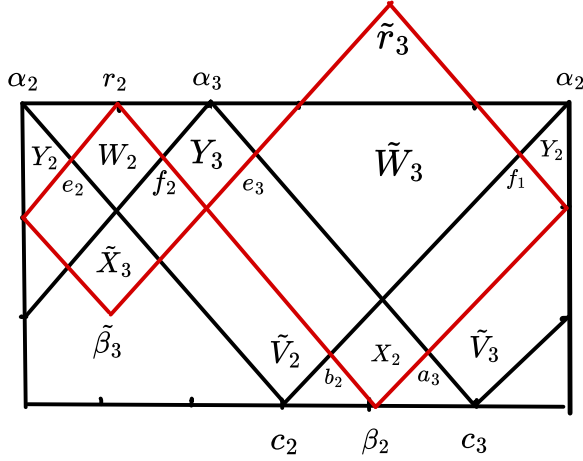
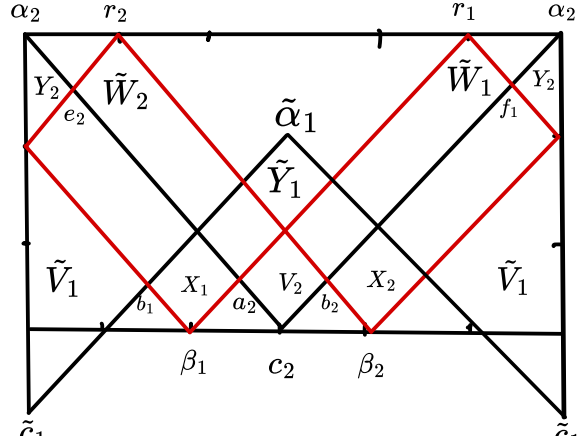


**Figure 5.** Illustration of the geometric structure used in deriving consequences of connected entanglement wedge  $\mathcal{E}(V_1 \cup \dots \cup V_n)$ . Panel (a) shows the geometric structure  $\mathcal{Z}_{in}$  (future horizon of  $\mathcal{E}(V_1 \cup \dots \cup V_n)$ ) cut by  $\partial J^-[E(Y_i)]$ , where future null sheets emanating from  $RT(X_i)$  are shown in red and past null sheets emanating from  $RT(Y_j)$  are shown in green. The curves  $C_i = \partial J^-[E(Y_i)] \cap \mathcal{Z}_{in}$  is shown as  $a_i - d_i - b_i$ . Panel (b) show the  $\mathcal{Z}_{in}$  in a flattened fashion where  $S_{V_i}$  is the intersection of null sheet  $\partial J^-[E(Y_i)]$  with  $\Sigma_1$ , i.e.  $S_{V_i} = \partial J^-[E(Y_i)] \cap \Sigma_1$ . Arrows indicate the direction along which null expansion  $\theta$  decreases. Panels (c) and (d) are similar to panels (a) and (b) but for enlarged input regions.



(a)



(b)

**Figure 6.** Illustration of modified input and output regions for  $n = 3$ . Panel (a) show that  $RT(Y_2) \cup RT(Y_3)$  can be regarded as HRRT surfaces of  $\mathcal{E}(W_2 \cup \tilde{W}_3)$ , where  $\tilde{W}_3 \supseteq W_3 \cup Y_1 \cup W_1$ . We get an effective  $c_2, c_3 \rightarrow r_2, \tilde{r}_3$  scattering. Panel (b) shows that  $RT(X_1) \cup RT(X_2)$  can be regarded as HRRT surfaces of  $\mathcal{E}(\tilde{V}_1 \cup V_2)$ , where  $\tilde{V}_1 \supseteq V_3 \cup X_3 \cup V_1$ . We get an effective  $\tilde{c}_1, c_2 \rightarrow r_1, r_2$  scattering. Note that in this case output regions are enlarged although output points  $r_1, r_2$  remain unchanged.

lies above

$$\mathcal{R}_{X_1, X_2} := \partial J^+[RT(X_1)] \cap \partial J^+[RT(X_2)].$$

Then the bulk geometry takes the form shown in Figure 5(c). Applying the standard focusing argument on null sheets emanating from extremal surfaces, using  $\theta \leq 0$  away from the extremal surface, yields

$$|RT(X_1)| + |RT(X_2)| \geq |RT(V_2)| + |RT(V_1 \cup X_1 \cup V_2)|. \quad (3.15)$$

This inequality contradicts the assumption that  $\mathcal{E}(X_1 \cup X_2)$  is disconnected. Therefore, the only consistent possibility is that the ridge  $\mathcal{R}_{\tilde{Y}_1, Y_2}$  lies below  $\mathcal{R}_{X_1, X_2}$ , or equivalently,

$$J^+[\mathcal{E}(X_1)] \cap J^+[\mathcal{E}(X_2)] \cap J^+[\mathcal{E}(Y_2)] \cap J^+[\mathcal{E}(\tilde{Y}_1)] = \emptyset. \quad (3.16)$$

Furthermore, we can improve (3.16) to

$$\mathcal{R}_{\tilde{Y}_1, Y_2} \cap \mathcal{E}(V_1 \cup V_2 \cup V_3) \neq \emptyset. \quad (3.17)$$

This follows from the observation that the null sheet  $\partial J^+[\mathcal{E}(\tilde{Y}_1)]$  lies to the past side of  $\partial J^+[\mathcal{E}(X_3)]$ , which can be shown using a similar argument as in Lemma 2.1.

**(Optional) scattering interpretation.** The regions  $X_1, X_2$  and  $\tilde{Y}_1, Y_2$  may be regarded as the causal complements of input and output regions in an effective 2-to-2 scattering process  $\tilde{c}_1, c_2 \rightarrow r_1, r_2$  (see Figure 6(b)), where the *modified input point*  $\tilde{c}_1$  is defined, along with the *modified input region*  $\tilde{V}_1$ , through

$$\hat{J}^+[\tilde{c}_1] \cap \hat{J}^-[r_1] \cap \hat{J}^-[r_2] = \tilde{V}_1 = (X_1 \cup V_2 \cup X_2)^c.$$

The corresponding output regions  $\tilde{W}_1, \tilde{W}_2$  are enlarged accordingly, while the output points  $r_1, r_2$  remain unchanged. This follows from entanglement wedge nesting together with the null sheet comparison theorem/maximum principle. First choose another bulk Cauchy slice  $\Sigma' \supseteq \gamma = RT(X_1 \cup V_2 \cup X_2)$  such that the curve  $\tilde{\gamma} = \partial J^+[\mathcal{E}(\tilde{Y}_1)] \cap \Sigma'$  has mean curvature pointing away from  $X_3$  (by making timelike second fundamental form of  $\Sigma$  at  $\tilde{\gamma}$  arbitrarily small and noting that null expansion pointing toward  $X_3$  is negative). Then maximum principle demands that  $\gamma$  being mean curvature zero on  $\Sigma'$

Note that  $\mathcal{E}(W_1 \cup \dots \cup W_n)$  being connected does not, by itself, guarantee that  $\mathcal{E}(\tilde{W}_1 \cup \tilde{W}_2)$  is connected. However, if we additionally assume that  $\mathcal{E}(\tilde{W}_1 \cup \tilde{W}_2)$  is connected, then (3.17) can be rephrased as<sup>7</sup>

$$\mathcal{E}(V_1 \cup V_2 \cup V_3) \cap \mathcal{E}(\tilde{W}_1 \cup \tilde{W}_2) \neq \emptyset. \quad (3.18)$$

In pairwise form, this reads

$$\mathcal{E}(\tilde{V}_1 \cup V_2) \cap \mathcal{E}(\tilde{W}_1 \cup \tilde{W}_2) \neq \emptyset. \quad (3.19)$$

---

<sup>7</sup>Strictly speaking, one must also ensure that the ridge  $\mathcal{R}_{\tilde{Y}_1, Y_2}$  enters  $\mathcal{E}(V_1 \cup V_2 \cup V_3)$ , rather than merely lying below  $\mathcal{R}_{X_1, X_2}$ . This follows from entanglement wedge nesting together with the null sheet comparison theorem; see Appendix A for details.

**Generalization to arbitrary  $n$ : pairwise entering ridges.** Repeating the same geometric construction and focusing calculation in the general  $n$ -to- $n$  lattice, one finds that pairwise disconnectedness of  $\mathcal{E}(X_i \cup X_j)$  forces the existence of auxiliary diamonds  $\tilde{Y}_i, \tilde{Y}_j$  such that the ridge enters  $\mathcal{E}(V_1 \cup \dots \cup V_n)$ :

$$\forall i \neq j, \quad \mathcal{E}(V_1 \cup \dots \cup V_n) \cap \mathcal{R}_{\tilde{Y}_i, \tilde{Y}_j} \neq \emptyset. \quad (3.20)$$

Here  $\tilde{Y}_i$  and  $\tilde{Y}_j$  are defined so that  $(\hat{J}^-[\tilde{Y}_i] \cap \hat{\Sigma}_1)'$  and  $(\hat{J}^-[\tilde{Y}_j] \cap \hat{\Sigma}_1)'$  yield Cauchy surfaces for the two components of  $(X_i \cup X_j)^c$ , ensuring that  $\partial J^-[\tilde{Y}_i] \cap \Sigma_1$  and  $\partial J^-[\tilde{Y}_j] \cap \Sigma_1$  are homologous to the HRRT surfaces of the two components of  $(X_i \cup X_j)^c$ .

### 3.2.3 A layered reduction from pairwise data to a top-level entering ridge

We now organize the general- $n$  consequences into a layered reduction on the boundary lattice. The guiding idea is to regroup boundary regions into effective scattering configurations, producing new auxiliary input points and new auxiliary output diamonds at each layer. The geometric output of each layer is the existence of an *entering ridge* for that effective configuration. Iterating this procedure culminates in an entering ridge for the original output diamonds  $Y_k$ .

**Layer 1.** Equation (3.20) is precisely the base-layer statement: for every pair  $i \neq j$  there exist auxiliary diamonds  $\tilde{Y}_i^{(1)}, \tilde{Y}_j^{(1)}$  whose ridge enters  $\mathcal{E}(V_1 \cup \dots \cup V_n)$ .

**Higher layers and the top layer.** At the next layer one regroups the boundary into alternating blocks  $X_a, \tilde{V}_a, X_{a+1}, \tilde{V}_{a+1}, \dots$  and defines new modified input points  $\tilde{c}_A^{(m)}$  by causal-diamond equalities of the form

$$\tilde{V}_A^{(m)} = \hat{J}^+(\tilde{c}_A^{(m)}) \cap \bigcap_{r \in \mathcal{R}_A} \hat{J}^-(r),$$

with  $\mathcal{R}_A$  the relevant collection of fixed output points for that block<sup>8</sup>, and defines new auxiliary output diamonds  $\tilde{Y}_A^{(m)}$  as the boundary diamonds associated to the antipodal points of the  $\tilde{c}_A^{(m)}$  on the lattice. Repeating the same contradiction/focusing comparison at each regrouping step shows that at every layer  $m$  there exists at least one ridge built from two of the  $\tilde{Y}_A^{(m)}$  that enters  $\mathcal{E}(V_1 \cup \dots \cup V_n)$ . After finitely many iterations, the auxiliary diamonds become the original  $Y_k$ , yielding the top-layer consequence

$$\exists k \neq l \quad \text{s.t.} \quad \mathcal{E}(V_1 \cup \dots \cup V_n) \cap \mathcal{R}_{Y_k, Y_l} \neq \emptyset, \quad (3.21)$$

which is the same entering-ridge statement as (3.8).

We summarize discussions in this section in the following theorem.

**Theorem 3.2** (Entering-ridge consequences of connected  $\mathcal{E}(V_1 \cup \dots \cup V_n)$ ). *Assume Assumption 1. If  $\mathcal{E}(V_1 \cup \dots \cup V_n)$  is connected, then:*

---

<sup>8</sup>Recall that each  $X_i$  are related to output point  $r_i$ . Therefore, a set of  $X_a$ 's remain unchanged implies that the corresponding output points remain unchanged.

1. (**Top-layer entering ridge.**) There exist  $k \neq l$  such that the ridge

$$\mathcal{R}_{Y_k, Y_l} := \partial J^-[RT(Y_k)] \cap \partial J^-[RT(Y_l)]$$

enters  $\mathcal{E}(V_1 \cup \dots \cup V_n)$ , equivalently

$$\mathcal{E}(Y_k^c) \cap \mathcal{E}(Y_l^c) \cap \mathcal{E}(V_1 \cup \dots \cup V_n) \neq \emptyset.$$

This is the geometric consequence (3.8).

2. (**Base-layer entering ridges from pairwise data.**) If in addition  $\mathcal{E}(X_i \cup X_j)$  is disconnected for all  $i \neq j$  (equivalently  $I(X_i : X_j) = 0$ ), then for every pair  $i \neq j$  there exist auxiliary boundary diamonds  $\tilde{Y}_i, \tilde{Y}_j$  constructed from the boundary lattice such that

$$\mathcal{E}(V_1 \cup \dots \cup V_n) \cap \mathcal{R}_{\tilde{Y}_i, \tilde{Y}_j} \neq \emptyset, \quad \mathcal{R}_{\tilde{Y}_i, \tilde{Y}_j} := \partial J^-[RT(\tilde{Y}_i)] \cap \partial J^-[RT(\tilde{Y}_j)].$$

Moreover, the past sets  $\partial J^-(\tilde{Y}_i) \cap \Sigma_1$  and  $\partial J^-(\tilde{Y}_j) \cap \Sigma_1$  are homologous to the HRRT surfaces of the two components of  $(X_i \cup X_j)^c$ .

3. (**Layered reduction.**) The entering-ridge statements in Item 2 can be iterated across successive regroupings of the boundary lattice (Section 3.2.3). At each layer one produces modified input points  $\tilde{c}^{(m)}$  (defined by causal-diamond equalities) and auxiliary output diamonds  $\tilde{Y}^{(m)}$ , such that at that layer there exists at least one ridge  $\mathcal{R}_{\tilde{Y}_A^{(m)}, \tilde{Y}_B^{(m)}}$  entering  $\mathcal{E}(V_1 \cup \dots \cup V_n)$ . After finitely many iterations, one recovers Item 1 for the original diamonds  $Y_k$ .

**(Optional scattering reformulation.)** If  $\mathcal{E}(W_1 \cup \dots \cup W_n)$  is also connected, then  $\mathcal{E}(Y_1 \cup \dots \cup Y_n)$  is fully disconnected, and for any  $k \neq l$  the two components  $\tilde{W}_k, \tilde{W}_l$  of  $(Y_k \cup Y_l)^c$  are given by (3.9) and admit output points  $\tilde{r}_k, \tilde{r}_l$  defined by (3.10)–(3.11). In this case, the entering-ridge statement in Item 1 can be equivalently expressed as

$$\mathcal{E}(V_1 \cup \dots \cup V_n) \cap \mathcal{E}(\tilde{W}_k \cup \tilde{W}_l) \neq \emptyset$$

for some  $k \neq l$ .

**Remark 3.3.** For  $n = 3$ , connectedness of  $\mathcal{E}(V_1 \cup V_2 \cup V_3)$  is equivalent to the two conditions in Remark 3.1. In particular, the pairwise condition  $I(X_i : X_j) = 0$  admits a direct interpretation in terms of excluding partially connected phases.

For  $n > 3$ , the situation is intrinsically multipartite: connectedness of  $\mathcal{E}(V_1 \cup \dots \cup V_n)$  imposes constraints not captured by pairwise statements alone. In the ridge language, this multipartite structure is naturally organized by the layered reduction of Section 3.2.3, which iteratively propagates “entering ridge” statements from auxiliary diamonds to the top-level ridge  $\mathcal{R}_{Y_k, Y_l}$  entering  $\mathcal{E}(V_1 \cup \dots \cup V_n)$ .

### 3.3 Generalized bulk scattering regions

In the 2-to-2 asymptotic scattering problem, a generalized bulk scattering region

$$\mathcal{S}_E = \mathcal{E}(V_1 \cup V_2) \cap \mathcal{E}(W_1 \cup W_2) \quad (3.22)$$

or the modified version

$$\tilde{\mathcal{S}}_E = [\mathcal{E}(V_1 \cup V_2) / (\mathcal{E}(V_1) \cup \mathcal{E}(V_2))] \cap [\mathcal{E}(W_1 \cup W_2) / (\mathcal{E}(W_1) \cup \mathcal{E}(W_2))] \quad (3.23)$$

was identified to characterize connectedness of  $\mathcal{E}(V_1 \cup \dots \cup V_n)$  and  $\mathcal{E}(W_1 \cup \dots \cup W_n)$ . Here we trivially generalize the above bulk scattering region as

$$\mathcal{S}_E = \mathcal{E}(V_1 \cup \dots \cup V_n) \cap \mathcal{E}(W_1 \cup \dots \cup W_n) \quad (3.24)$$

and discuss necessary conditions for  $\mathcal{S}_E \neq \emptyset$ .

**Theorem 3.4.** *Assume the standard conditions listed in Assumption 1. If  $\mathcal{E}(V_1 \cup \dots \cup V_n)$  and  $\mathcal{E}(W_1 \cup \dots \cup W_n)$  are connected and furthermore,*

$$\mathcal{E}(V_1 \cup \dots \cup V_n) \cap \mathcal{E}(Y_i^c) \cap \mathcal{E}(Y_j^c) \neq \emptyset, \quad \forall i \neq j, \quad (3.25)$$

*then  $\mathcal{S}_E \neq \emptyset$ .*

*We can recast the condition (3.25) in terms of enlarged output regions as*

$$\mathcal{E}(V_1 \cup \dots \cup V_n) \cap \mathcal{E}(\tilde{W}_i \cup \tilde{W}_j) \neq \emptyset, \quad \forall i \neq j, \quad (3.26)$$

*where  $\tilde{W}_i \cup \tilde{W}_j = (Y_i \cup Y_j)^c$ .*

**Remark 3.5.** *In particular, one can use focusing calculations, which should be very familiar by now, to show that if  $I(V_i : V_j) > 0, \forall i \neq j$  or if  $V_i$ 's have pairwise connected entanglement wedges, then (3.25) is necessarily satisfied.*

*Proof.* We first note that  $\mathcal{E}(V_1 \cup \dots \cup V_n) \cap \mathcal{E}(W_1 \cup \dots \cup W_n) \neq \emptyset$  is equivalent to the future horizon of  $\mathcal{E}(V_1 \cup \dots \cup V_n)$  and the past horizon of  $\mathcal{E}(W_1 \cup \dots \cup W_n)$  intersects because both  $\mathcal{E}(V_1 \cup \dots \cup V_n)$  and  $\mathcal{E}(W_1 \cup \dots \cup W_n)$  are compact sets in  $\overline{M}$ .

We use a similar geometric structure as before. Consider the upper horizon of  $\mathcal{E}(V_1 \cup \dots \cup V_n)$  or  $\mathcal{Z}_{in}$  in the notation of section 3.2. As argued above,  $\mathcal{N}_{Y_i} = \partial J^+[\mathcal{E}(Y_i)]$  intersect  $\mathcal{Z}_{in}$  at a simple curve  $\mathcal{C}_i$ , with endpoints of  $\partial V_i$ , i.e.  $a_i$  and  $b_i$ . Moreover,  $\mathcal{C}_i$  together with the boundary future horizon  $\hat{H}^+[V_i]$  of  $V_i$  bounds a compact set  $D_i$  on  $\mathcal{Z}_{in}$ , which is topologically a disk. An important feature is that  $D_i$ 's are arranged cyclically on  $\mathcal{Z}_{in}$  since  $V_i$  are arranged cyclically on  $\partial M$ . The condition (3.25) states that  $D_i \cap D_j \neq \emptyset$  for all pairs  $i \neq j$ . We only need to prove the claim that pairwise intersections among  $D_i$ 's imply common intersections among all  $D_i$ 's.

We proceed by induction. When  $n = 2$ , the claim is trivially true. Suppose the claim holds for  $n$ , we need to show that it holds for  $n + 1$ .

By induction hypothesis,  $D_c = D_1 \cap \dots \cap D_n \neq \emptyset$ . Suppose  $D_{n+1} \cap D_c = \emptyset$ . Then  $D_{n+1}$  lies in between  $D_c$  and  $\hat{H}^+[V_{n+1}]$ . Since  $D_C$  results from intersecting the first  $n$  sets,

its boundary  $\partial D_c$  is composed of segments from the boundaries  $\partial D_k$  of the constituent sets. The condition  $D_c \cap D_{n+1} = \emptyset$  implies that  $D_{n+1}$  lies entirely outside  $D_c$ . Given the specific convex structure of our setup (where each  $D_i$  is a subset of intersecting null sheets), this forces  $D_{n+1}$  and  $D_c$  to be separated by at least one full boundary component. Consequently, there must exist at least one set  $D_k$  (for  $1 \leq k \leq m$ ) whose boundary contributes a segment to  $\partial D_c$  that completely separates  $D_c$  from  $D_{n+1}$ . For such a  $D_k$ , it follows geometrically that  $D_k \cap D_{n+1} = \emptyset$ . This directly contradicts our initial assumption that all pairs  $D_i \cap D_j \neq \emptyset$ .  $\square$

## 4 Conclusion and Discussion

Similar to the proofs of CWT and  $n$ -to- $n$ , the proofs given here will also work for semiclassical spacetimes that satisfy the quantum maximin formula [20] and the quantum focusing conjecture [21].

The configuration of disjoint input regions  $V_1 \cup \dots \cup V_n$  fully specifies the boundary setup for the asymptotic  $n$ -to- $n$  scattering problem. Consequently, the results derived here apply generally to the entanglement wedge structure of multipartite, spacelike-separated boundary regions with shape of causal domains (not allowing adjacent regions).

### 4.1 An observation about different generalizations of the 2-to-2 Connected Wedge Theorem

We make an observation that would help to understand relations among different generalizations of the 2-to-2 and  $n$ -to- $n$  connected wedge theorems.

We noted that there are two null sheets anchored to  $\hat{J}^+[c_i]$  appeared in the proofs: the future-pointing null sheet  $\mathcal{N}_{V_i}$  emanating from  $RT(V_i)$  and the past-pointing null sheet  $\mathcal{N}_{Y_i}$  emanating from  $RT(Y_i)$ . Similarly, for  $\hat{J}^+[\beta_i]$ , we would consider the future-pointing null sheet  $\mathcal{N}_{X_i}$  emanating from  $RT(X_i)$  and the past-pointing null sheet  $\mathcal{N}_{W_i}$  emanating from  $RT(W_i)$ .

One can argue for an positioning relation between  $\mathcal{N}_{V_i}$  and  $\mathcal{N}_{Y_i}$  with the same  $i$ . See Figure 7 for an illustration. First note that the future pointing null sheet  $\mathcal{N}_{V_i}$  from  $RT(V_i)$  is the future horizon of  $\mathcal{E}(V_i^c)$ . On the boundary  $\partial M$ ,  $\hat{D}[V_i^c]$  contains  $Y_i$  (since  $Y_i \subseteq \hat{J}^+[\alpha_i]$  and  $\alpha_i$  is antipodal point of  $c_i$ ), thus  $\mathcal{E}(Y_i) \subseteq \mathcal{E}(V_i^c)$  by entanglement wedge nesting. This implies that  $RT(Y_i)$  is spacelike separated from  $\mathcal{N}_{V_i}$  and moreover,  $RT(Y_i)$  lies closer to  $Y_i$  than  $\mathcal{N}_{V_i} \cap \Sigma_2$ . Similarly, the past null sheet  $\mathcal{N}_{Y_i}$  is the past horizon of  $\mathcal{E}(Y_i^c)$  and  $\mathcal{E}(Y_i^c) \supseteq \mathcal{E}(V_i)$ . This implies that  $RT(V_i)$  is spacelike separated from  $\mathcal{N}_{Y_i}$  and moreover,  $RT(V_i)$  lies closer to  $V_i$  than  $\mathcal{N}_{Y_i} \cap \Sigma_1$ . To sum up, we have two null sheets,  $\mathcal{N}_{V_i}$  and  $\mathcal{N}_{Y_i}$ , coinciding on  $\partial M$ , with one lying to a specific side relative to the other at  $\Sigma_1$  and  $\Sigma_2$ :  $\mathcal{N}_{V_i}$  lies closer to  $V_i$  (or closer to  $\partial M$ ) than  $\mathcal{N}_{Y_i}$  on  $\Sigma_1$  while  $\mathcal{N}_{Y_i}$  lies closer to  $Y_i$  (or closer to  $\partial M$ ) than  $\mathcal{N}_{V_i}$  on  $\Sigma_2$ . If they intersect in the bulk and do not coincide everywhere, then their intersection would necessarily contain either multiple connected components or a closed loop. Both possibilities are excluded by the same separation and generator-uniqueness argument used in Lemma 2.1. To avoid contradiction with causality, they have empty intersection or coincide completely. One can also derive this fact from the maximum

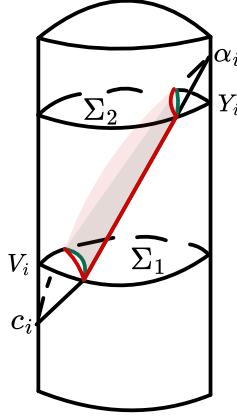


**Figure 7.** Illustration of position relation between  $\mathcal{N}_{V_i}$  and  $\mathcal{N}_{Y_i}$ . The red sheet or curves are associated with  $\mathcal{N}_{V_i} = \partial J^+[RT(V_i)]$ . The green sheet or curves are associated with  $\mathcal{N}_{Y_i} = \partial J^-[RT(Y_i)]$ . The points  $c_i$  and  $\alpha_i$  are antipodal points.

principle using a similar argument as in refs. [22] or [19]. A similar reasoning would show that  $\mathcal{N}_{X_i}$  and  $\mathcal{N}_{W_i}$  either coincide completely or have empty intersection. Specifically,  $\mathcal{N}_{X_i}$  lies closer to  $X_i$  than  $\mathcal{N}_{W_i}$  (or equivalently  $\mathcal{N}_{W_i}$  lies closer to  $W_i$  than  $\mathcal{N}_{X_i}$ ).

In the generalized 2-to-2 Connected Wedge Theorem by ref. [23], a bulk region

$$\mathcal{S}'_E = J^+[\mathcal{E}(V_1)] \cap J^+[\mathcal{E}(V_2)] \cap J^-[\mathcal{E}(W_1)] \cap J^-[\mathcal{E}(W_2)] \quad (4.1)$$

is used, whose nonemptiness was shown to imply connectedness of  $\mathcal{E}(V_1 \cup V_2)$ . On the other hand, in the generalized 2-to-2 Connected Wedge Theorem by refs. [11, 12, 24], another bulk region

$$\mathcal{S}_E = \mathcal{E}(V_1 \cup V_2) \cap \mathcal{E}(W_1 \cup W_2) \quad (4.2)$$

is used, whose nonemptiness was shown to follow from connectedness of  $\mathcal{E}(V_1 \cup V_2)$  and  $\mathcal{E}(W_1 \cup W_2)$ .

The bulk region  $\mathcal{S}'_E$  involves  $\mathcal{N}_{V_i}$  and  $\mathcal{N}_{W_i}$  while the bulk region  $\mathcal{S}_E$  involves  $\mathcal{N}_{Y_i}$  and  $\mathcal{N}_{X_i}$ . The above observation on the inclusion relation between  $\mathcal{N}_{V_i}$  and  $\mathcal{N}_{Y_i}$  or between  $\mathcal{N}_{X_i}$  and  $\mathcal{N}_{W_i}$  would immediately imply that

$$\mathcal{S}'_E \subseteq \mathcal{S}_E, \quad (4.3)$$

as one would expect from the two generalization of the 2-to-2 Connected Wedge Theorem.

A similar remark applies to the  $n$ -to- $n$  scattering problem discussed here. The bulk region

$$J^+[\mathcal{E}(V_i)] \cap J^+[\mathcal{E}(V_j)] \cap J^-[\mathcal{E}(W_k)] \cap J^-[\mathcal{E}(W_l)], \quad , i \neq j, k \neq l$$

involved in the necessary condition (Theorem 1.3) is contained in the bulk region

$$J^-[RT(Y_k)] \cap J^-[RT(Y_l)] \cap J^+[\mathcal{E}(X_i)] \cap J^+[\mathcal{E}(X_j)]$$

in the sufficient condition (Theorem 3.2).

## 4.2 Future Directions

For multipartite  $n > 2$  scattering processes, the holographic dictionary appears less transparent than in the  $n = 2$  case. In particular, the condition  $\mathcal{S}_E \neq \emptyset$  seems more restrictive than the mere connectedness of  $\mathcal{E}(V_1 \cup \dots \cup V_n)$  and  $\mathcal{E}(W_1 \cup \dots \cup W_n)$ . Our analysis addresses this increased complexity by reducing the problem to a pairwise framework and yields several concrete geometric consequences. This reduction is justified by the intrinsic structure of holographic states, which are highly constrained and, in particular, cannot support purely GHZ-like multipartite entanglement [25].

While the results presented here do not yet constitute a complete or equivalent geometric characterization for  $n > 2$ , they significantly extend the core principle established for 2-to-2 scattering: nontrivial boundary quantum protocols are faithfully encoded in specific, nonlocal geometric signatures in the bulk spacetime. A fully equivalent characterization for general  $n$  will likely require genuinely multipartite information-theoretic tools. In this regard, Theorem 2.11 provides a complete information-theoretic characterization of when the entanglement wedge of multiple disjoint spacelike-separated regions is connected. We leave further exploration along these lines to future work.

In this paper, we focused on identifying necessary as well as sufficient conditions for the connectedness of multipartite entanglement wedges. An alternative and complementary perspective would be to formulate necessary or sufficient conditions directly for the existence of bulk-only scattering processes [7], namely configurations satisfying

$$\bigcap_i J^+[c_i] \cap \bigcap_j J^-[r_j] \neq \emptyset \quad \text{while} \quad \bigcap_i \hat{J}^+[c_i] \cap \bigcap_j \hat{J}^-[r_j] = \emptyset. \quad (4.4)$$

Finally, it would also be interesting to generalize the discussions in this work to higher-dimensional asymptotically AdS spacetimes.

## Acknowledgments

I thank Edward Witten for getting me interested in this subject and Shing-Tung Yau for his enduring support.

## References

- [1] J. Maldacena, *The large- $N$  limit of superconformal field theories and supergravity*, *International journal of theoretical physics* **38** (1999) 1113.
- [2] E. Witten, *Anti de Sitter space and holography*, *arXiv preprint hep-th/9802150* (1998) .
- [3] S. Gao and R.M. Wald, *Theorems on gravitational time delay and related issues*, *Classical and Quantum Gravity* **17** (2000) 4999.
- [4] M. Gary, S.B. Giddings and J. Penedones, *Local bulk S-matrix elements and conformal field theory singularities*, *Physical Review D—Particles, Fields, Gravitation, and Cosmology* **80** (2009) 085005.
- [5] I. Heemskerk, J. Penedones, J. Polchinski and J. Sully, *Holography from conformal field theory*, *Journal of High Energy Physics* **2009** (2009) 079.

- [6] J. Penedones, *Writing CFT correlation functions as AdS scattering amplitudes*, *Journal of High Energy Physics* **2011** (2011) 1.
- [7] J. Maldacena, D. Simmons-Duffin and A. Zhiboedov, *Looking for a bulk point*, *Journal of High Energy Physics* **2017** (2017) 1.
- [8] A. May, G. Penington and J. Sorce, *Holographic scattering requires a connected entanglement wedge*, *Journal of High Energy Physics* **2020** (2020) 1.
- [9] S. Ryu and T. Takayanagi, *Holographic derivation of entanglement entropy from the anti-de Sitter space/conformal field theory correspondence*, *Physical review letters* **96** (2006) 181602.
- [10] V.E. Hubeny, M. Rangamani and T. Takayanagi, *A covariant holographic entanglement entropy proposal*, *Journal of High Energy Physics* **2007** (2007) 062.
- [11] B. Zhao, *A proof of generalized connected wedge theorem*, *JHEP* **2025** (2025) xxx [[2509.23119](#)].
- [12] C. Lima, S. Pasterski and C. Waddell, *On sufficient conditions for holographic scattering*, *arXiv preprint arXiv:2509.26264* (2025) .
- [13] A. May, J. Sorce and B. Yoshida, *The connected wedge theorem and its consequences*, *Journal of High Energy Physics* **2022** (2022) 1.
- [14] R.M. Wald, *General relativity*, University of Chicago press (2024).
- [15] M. Headrick, V.E. Hubeny, A. Lawrence and M. Rangamani, *Causality & holographic entanglement entropy*, *Journal of High Energy Physics* **2014** (2014) 1.
- [16] E. Witten, *A mini-introduction to information theory*, *La Rivista del Nuovo Cimento* **43** (2020) 187.
- [17] E. Witten, *Introduction to black hole thermodynamics*, *The European Physical Journal Plus* **140** (2025) 430.
- [18] S. Hernández-Cuenca, V.E. Hubeny and H.F. Jia, *Holographic entropy inequalities and multipartite entanglement*, *Journal of High Energy Physics* **2024** (2024) 1.
- [19] A.C. Wall, *Maximin surfaces, and the strong subadditivity of the covariant holographic entanglement entropy*, *Classical and Quantum Gravity* **31** (2014) 225007.
- [20] C. Akers, N. Engelhardt, G. Penington and M. Usatyuk, *Quantum maximin surfaces*, *Journal of High Energy Physics* **2020** (2020) 1.
- [21] R. Bousso, Z. Fisher, S. Leichenauer and A.C. Wall, *Quantum focusing conjecture*, *Physical Review D* **93** (2016) 064044.
- [22] G.J. Galloway, *Maximum principles for null hypersurfaces and null splitting theorems*, *arXiv preprint math/9909158* (1999) .
- [23] A. May, *Holographic quantum tasks with input and output regions*, *Journal of High Energy Physics* **2021** (2021) 1.
- [24] S. Leutheusser and H. Liu, *Superadditivity in large N field theories and performance of quantum tasks*, *Physical Review D* **112** (2025) 046001.
- [25] V. Balasubramanian, M.J. Kang, C. Cummings, C. Murdia and S.F. Ross, *Purely GHZ-like entanglement is forbidden in holography*, *arXiv preprint arXiv:2509.03621* (2025) .